Journal of Anatomy

J. Anat. (2010) **217**, pp76–82 doi: 10.1111/j.1469-7580.2010.01237.x

METHODS

Characterization of eight different tetracyclines: advances in fluorescence bone labeling

Christoph Pautke,[1] Stephan Vogt,[2] Kilian Kreutzer,[3] Cornelia Haczek,[3,4] Gabriele Wexel,[4] Andreas Kolk,[3] Andreas B. Imhoff,[2] Horst Zitzelsberger,[5] Stefan Milz[6,7] and Thomas Tischer[2,6,8]

[1]*Department of Oral and Maxillofacial Surgery, University of Munich, Munich, Germany*
[2]*Departments of Orthopedic Surgery and Orthopedic Sport Surgery, TUM, Munich, Germany*
[3]*Department of Oral and Maxillofacial Surgery, Technische Universität München, Munich, Germany*
[4]*Institute of Experimental Oncology and Therapy Research, Technische Universität München, Munich, Germany*
[5]*Institute of Molecular Radiation Biology, Helmholtz Center Munich: German Research Center for Environmental Health, Neuherberg, Germany*
[6]*Department of Anatomy, University of Munich, Munich, Germany*
[7]*AO Research Institute, AO Foundation, Davos, Switzerland*
[8]*Department of Orthopaedics, University of Rostock, Rostock, Germany*

Abstract

Polychrome sequential labeling with fluorochromes is a standard technique for the investigation of bone formation and regeneration processes *in vivo*. However, for human application, only tetracycline and its derivates are approved as fluorochromes. Therefore, the aim of this study was to determine the fluorescence characteristics of the different tetracycline derivates to assess the feasibility of sequential *in vivo* bone labeling using distinguishable fluorochromes. Eight different tetracycline derivates were injected subcutaneously into growing rats as a single dose or sequentially in different combinations. After preparation of resin-embedded undecalcified bone sections, the fluorescence properties of the tetracycline derivates in bone were analyzed using conventional fluorescence microscopy, spectral image analysis and confocal laser scanning microscopy. Each tetracycline derivate exhibited a characteristic fluorescence spectrum, but the differences between them were small. Chlortetracycline could be discriminated reliably from all other derivates and could therefore be combined with any other tetracycline derivate for reliably distinguishable double labeling. Tetracycline itself exhibited the brightest fluorescence of all the investigated derivates. Interestingly, in conventional microscopy the same tetracycline derivative can appear in different colours to the human eye, even if spectral analysis confirmed identical emission peaks. In conclusion, the data suggest that fluorescence double labeling of bone is feasible using appropriate tetracycline derivates in combination with spectral imaging modalities.

Key words bone histomorphometry; bone labeling; confocal laser scanning microscopy; fluorescence; polychrome sequence labeling; spectral image analysis; tetracycline.

Introduction

Tetracycline-based histological analysis of bone remodeling (Frost, 1969) is used routinely to address calcified tissue-related questions such as renal osteodystrophy (Coen et al. 2006), osteogenesis imperfecta (Rauch et al. 2000; Land et al. 2007), hyperparathyroidism (Rauch, 2006), osteomalacia (Rauch, 2006), bisphosphonate-induced changes of bone metabolism (Pautke et al. 2009, 2010) and normal bone metabolism (Schnitzler & Mesquita, 2006; Rauch et al. 2007). Due to their high affinity for calcium the tetracyclines are incorporated at the site of active mineralization of hydroxyapatite (Frost, 1963; Rahn, 1976). To generate parallel fluorochrome bands, the same tetracycline derivate is injected twice with a 10-day interval between injections, allowing morphometric measurements. Although the use of tetracycline derivates in clinical applications was introduced decades ago (Harris, 1960; Frost, 1969), to date detailed information on the fluorescence properties of the different tetracycline derivates in bone remain elusive. This is surprising because such information is highly important,

Correspondence
PD Dr. Dr. Christoph Pautke, Department of Oral and Maxillofacial Surgery, University of Munich, Lindwurmstr. 2a, D-80337 Munich, Germany. T: + 49 (0)89 51602919; F: +49 (0)321 21007467; E: christoph.pautke@gmx.net

Accepted for publication *17 March 2010*
Article published online *27 April 2010*

as tetracycline derivates are the only fluorochromes approved for human *in vivo* application.

In recent years, more sensitive detection methods have been developed. Spectral image analysis (Pautke et al. 2005) and confocal laser scanning microscopy (CLSM) (Jones et al. 2005; Maggiano et al. 2006; Smith et al. 2006; Pilolli et al. 2008) allow a better discrimination of the fluorescence emission characteristics than the naked eye can provide.

The need for an improvement in bone-labeling procedures is advocated by many authors (Rauch, 2006; Pautke et al. 2007; Pilolli et al. 2008) and, recently, a double-labeling technique using two different tetracycline derivates (tetracycline and demeclocycline) was proposed, but only conventional microscopic methods were employed (Lindsay et al. 2006). The ability to perform tetracycline bone labeling in human patients with two different fluorochromes instead of one would represent an important improvement. Two different fluorochromes, instead of one, would allow assessment of bone mineralization, and thus bone formation, at more than one time point. This is of particular interest in different fields of bone research, e.g. in the osseointegration of implants (Degidi et al. 2005), bone substitute materials or tissue-engineered bone remodeling in humans, or various questions regarding bone turnover affected by metabolic/systemic diseases (Freemont et al. 2005; Togawa et al. 2005; Land et al. 2007). Therefore, the aim of this study was to determine the fluorescence characteristics of eight different tetracycline derivates to test the feasibility of sequential *in vivo* tetracycline bone labeling.

Materials and methods

Tetracycline-derived fluorochromes

Eight different tetracycline derivates were used for this study: chlortetracycline, demeclocycline, doxycycline, methacycline, minocycline, oxycycline, rolitetracycline, and tetracycline. Details of the fluorochromes are given in Table 1. Prior to *in vivo* application, all fluorochromes were investigated for their fluorescence characteristics *in vitro*. Freshly harvested bone specimens from rat femur were incubated in tetracycline solutions (Aaron et al. 1984) and subsequently analyzed (each $n = 3$) using a spectrometer (Fluorolog, HORIBA Jobin Yvon Inc., Edison, NJ, USA, provided by the Faculty for Physics of the LMU Munich). The spectrometer measures the emission wavelength spectrum with a spatial resolution of 0.5 nm. The spectral data gained in the *in vitro* model were used for the verification of the spectra acquired with the spectral camera and the CLSM (confocal laser scanning microscopy). For animal application, the tetracyclines were dissolved in physiological saline solution, adjusted to neutral pH-values (pH 7.4) and sterilized by filtration before application. The tetracyclines were dissolved at a concentration such that a maximum volume of 1.5 mL was subcutaneously injected. An intravenous or subcutaneous fluorochrome application is more reliable in animals to achieve comparable dosages and sharper fluorescent bands (von Gaalen et al. 2010). Of the eight tetracycline derivates used, only two (oxytetracycline and doxycycline) are approved for intravenous application in humans by the Federal Drug Administration (FDA). Six of eight derivates are approved for human use as oral drugs (demeclocycline, methacycline, minocycline, tetracycline, and additionally oxytetracycline and doxycycline). Oral drug administration is unsafe due to the unpredictable uptake and bioavailability, in particular in animals. Chlortetracycline is only approved for a local administration and rolitetracycline is not approved for human applications at all.

For this basic science research the authors intended to compare many different tetracycline derivates that generally reveal a suitable fluorescence spectrum. Therefore, a subcutaneous injection was chosen as a reliable standard administration method.

Animal model

Twenty-four 5-week-old male Wistar rats with open femoral epiphyseal plates weighing approximately 200 g were employed for this study. Tetracycline was administered separately as a subcutaneous single-dose injection to achieve sharper fluorescence bands (van Gaalen et al. 2010): chlortetracycline $n = 3$, demeclocycline $n = 1$, doxycycline $n = 3$, methacycline $n = 1$, minocycline $n = 2$, oxycycline $n = 1$, rolitetracycline $n = 1$ and tetracycline $n = 1$. In addition, minocycline was also given orally ($n = 2$) due

Table 1 Chemical and spectral details including source and peak emission wavelength of the different tetracycline derivates in undecalcified bone sections. All fluorochromes were administered subcutaneously at a dose of 30 mg kg^{-1} bodyweight. Due to the weak fluorescence signal of chlortetracycline and doxycycline, a higher dose of 60 mg kg^{-1} bodyweight was administered for both derivates. Emission spectrum for minocycline was detectable only *in vitro* and not in the tissue.

Derivate	Source	Cat.-No.	Molecular formula	Molecular weight	Peak emission wave length [nm]
Chlortetracycline	Fluka	26430	$C_{22}H_{23}ClN_2O_8$ HCl	515.34	506
Demeclocycline	Sigma-Aldrich	D6140	$C_{21}H_{21}ClN_2O_8$	501.31	535
Doxycycline	Sigma-Aldrich	D9891	$C_{22}H_{24}N_2O_8$	512.94	529
Methacycline	Sigma-Aldrich	37906	$C_{22}H_{22}N_2O_8$	478.88	541
Minocycline	Sigma-Aldrich	M9511	$C_{23}H_{27}N_3O_7$	493.94	(521)
Oxytetracycline	Fluka	75966	$C_{22}H_{24}N_2O_9$	496.89	547
Rolitetracycline	Sigma-Aldrich	R2253	$C_{27}H_{33}N_3O_8$	527.57	529
Tetracycline	Sigma-Aldrich	T3383	$C_{22}H_{24}N_2O_8$	480.90	529

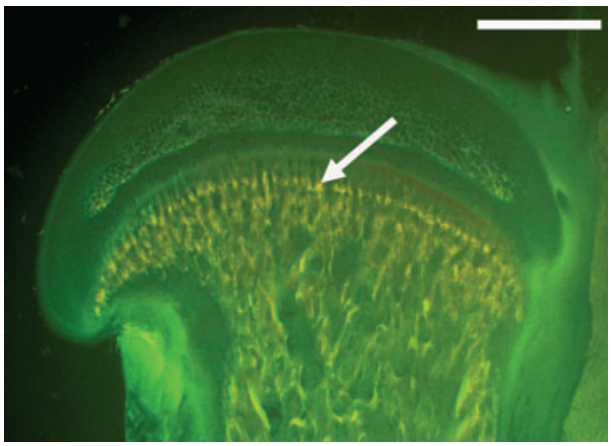

Fig. 1 Microscopic image of a sagittal rat femur section fluorescence picture (bar = 1 mm) using a green fluorescence filter set (#09, Zeiss; excitation 450–490 nm, beam splitter/emission 515 nm). Arrow shows area for further analysis.

to unexpected labeling results (see below). Animals were sacrificed 3 days after the fluorochrome administration and tissues were processed as described below to acquire the fluorescence spectrum of each single tetracycline derivate.

After spectral analysis of each tetracycline derivate, different combinations of several tetracycline derivates were investigated using three (doxy/chlor/tetra, $n = 2$), four (oxy/doxy/demeclo/chlor, $n = 3$; roli/chlor/doxy/metha, $n = 2$) or all eight tetracycline derivates ($n = 2$). The tetracyclines were administered at 3-day intervals (see Table 1). All tetracyclines were given at 30 mg kg^{-1} bodyweight except for chlortetracycline and doxycycline, which were given at 60 mg kg^{-1} bodyweight because of weak fluorescence labeling after analysis of the first labeling results.

Three days after the last tetracycline administration the animals were sacrificed by an intraperitoneal overdose of pentobarbitone sodium. Immediately thereafter, the femora were harvested and prepared for embedding: specimens were fixed in methanol for 4 days at 4 °C, kept in acetone for 2 days and then block-embedded in methylmethacrylate over a period of 12 days. Each specimen was cut into 100-μm-thick sections using a saw microtome (Leica SP 1600; Leitz, Wetzlar, Germany). Analysis was performed in the epiphysis of the proximal femur (Fig. 1). All animal experiments were carried out with the permission of the Bavarian government (animal experiment number AZ 55.2-1-54-2531-73-06).

Conventional fluorescence microscopy

Bone sections were analyzed using a microscope (Axioplan 2; Zeiss, Germany) in epifluorescence mode with an HBO 100 mercury lamp. A long-pass emission filter (filter set no. 01; Zeiss, see Fig. 3), a filter set for green fluorescence (filter set no. 09; Zeiss, details in the legend of Fig. 2), and a triple band filter set for green, red and infrared [SKY; Applied Spectral Imaging (ASI), Israel] were used. The authors did not have the permission of the company to publish details of the SKY filter set.

Spectral image acquisition and image analysis

Fluorescence images were analyzed using a Sagnac type interferometer (SpectralCube SD-300; ASI), which is installed on the microscope. The principles of the data acquisition process have been published previously (Malik et al. 1996; Pautke et al. 2005).

For image analysis, SpectraView Software (ASI) was used for linear unmixing (i.e. spectral decomposition) of the fluorescent signal. The system settings were chosen so that the complete emission spectrum of each tetracycline could be assessed (350–830 nm). To establish a practicable analysis algorithm which covers the full emission spectrum with an accuracy of 3-nm steps, image acquisition times of approximately 150 s and a raw image size of less than 100 megabytes were used. Measurements were carried out on three different bone sections at five different regions. The reference spectra of each tetracycline derivate were obtained from the same bone section in regions where labels did not overlap. By doing so, a spectral library was generated. After definition and subtraction of the background fluorescence the different tetracycline spectra were decomposed in their spectral components using the software. If one tetracycline spectrum (not only the peak but the complete curve) differs sufficiently from the background fluorescence, the respective

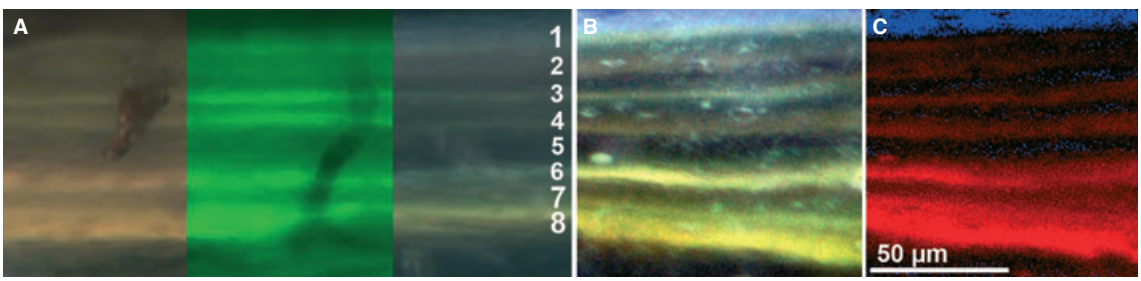

Fig. 2 (A) Fluorescence labeling with eight different tetracycline derivates using different fluorescence filter sets for green/red/infrared [SKY, Applied Spectral Imaging, Israel (no permission to publish filter details)], green (#09, Zeiss; excitation 450–490 nm, beam splitter/emission 515 nm) as well as a long-pass emission filter (#01 Zeiss; for details see Fig. 3). Note that doxycycline and rolitetracycline appear in different colours, but reveal a very similar emission spectra with the same wavelength peak (see Fig. 3). (B) Spectral image acquisition of the same bone area using a long-pass emission filter. Note that the tetracycline bands are more discernible. (C) By linear unmixing and false colour depiction, chlortetracycline (blue) can be distinguished and depicted separately from the other fluorochromes (red). 1: chlortetracycline; 2: methacycline; 3: tetracycline; 4: rolitetracycline; 5: minocycline; 6: oxycycline; 7: demeclocycline; 8: doxycycline.

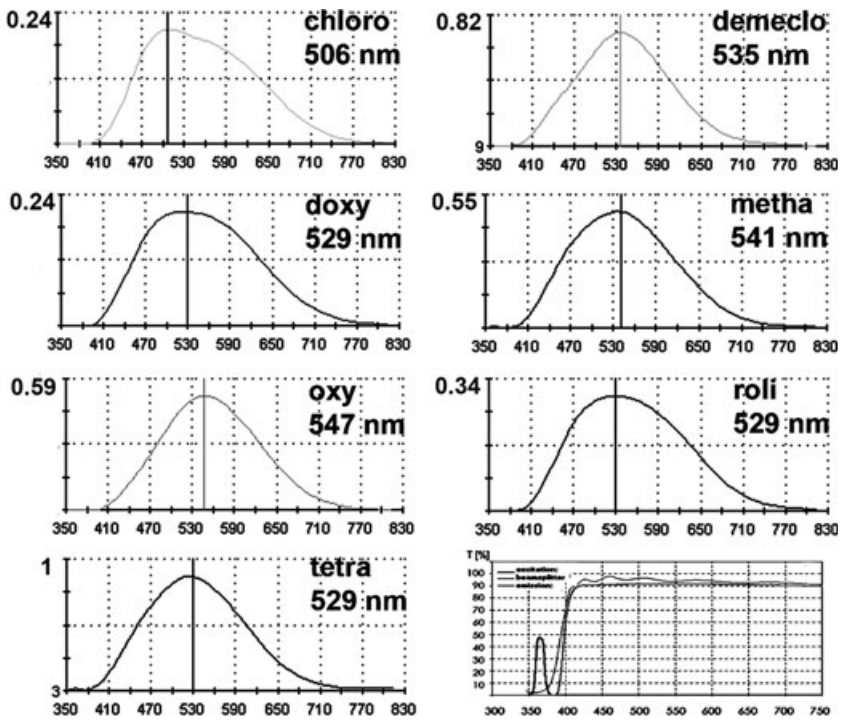

Fig. 3 *In vivo* wavelength characteristics of the applied tetracycline derivates in bone using a long-pass emission filter set. The characteristic details of the Zeiss filter set 01 are displayed in the lower righthand picture. The ordinate displays the relative values of fluorescence intensity compared to tetracycline. Minocycline showed no fluorescence *in vivo* and was therefore omitted.

fluorochrome-labeled region can be delineated and displayed in pseudo-colour, allowing morphometric measurement.

Confocal laser scanning microscopy and image analysis

Confocal laser scanning microscopy (CLSM) was performed using an LSM 510 META NLO with a Plan-Apochromat 20 × /0.5 objective (Zeiss, Germany; provided by the LMC ETH Zurich) and 458-nm argon laser (optimal excitation of all tetracyclines). For image acquisition the META detector (Zeiss) and for image analysis the LSM 5 Image Analyser Software (Zeiss) were used. First, lambda stacks, which comprise the whole emission spectrum of each tetracycline, were acquired and compiled into a fluorochrome database. Secondly, the signatures of the spectra of the polychrome-labeled specimens were compared either individually with the fluorochrome database, or the software automatically extracted the most reliable spectra (automatic component extraction). This was followed by linear unmixing, which resulted in a pseudo-colour picture for each fluorochrome. Using this procedure, it is possible to extract up to eight fluorochromes on the basis of their emission spectra signature over a band width of 100 nm. This approach is useful for the separation of fluorochromes with similar peak emission values but different spectral emission curves. Due to the demands of poly fluorescence and the short time interval between fluorochrome applications, a 450 × 450-μm region of interest was chosen. The images were acquired at a resolution of 512 × 512 pixels with an 8-bit depth of information per pixel. After fusion of the monochromatic pseudo-colour images, the morphometric measurements were carried out.

Results

The different tetracycline derivates could not be distinguished and in particular could not be depicted individually using conventional fluorescence filter sets (Fig. 2). All eight tetracycline derivates showed detectable fluorescence *in vitro* but only seven of them *in vivo* (Table 1; Fig. 3). Unexpectedly, minocycline failed to exhibit fluorescence levels *in vivo* after combined oral and subcutaneous administration. Nevertheless, *in vitro* spectral examination of the emitted light showed a detectable peak value at 521 nm and the typical emission curve of minocycline.

Using spectral image analysis, each of the other seven derivates presented a characteristic fluorescence spectrum after *in vivo* application with slightly different wavelength emission characteristics. Details of the fluorochrome properties are given in Table 1 and Fig. 3. Small inter-individual differences of the peak wavelength of each tetracycline derivate were observed, but these were within the accuracy of the spectral camera of ± 3 nm. The results were confirmed by confocal laser scanning microscopy.

Interestingly, the same tetracycline derivate in different regions appeared as slightly different fluorescence colours to the naked eye. In areas of new bone formation, fluorescence was less intense (most likely due to the lower calcium content of the newly formed osteoid) and appeared with redder fluorescence (Fig. 4). However, spectral fluorescence

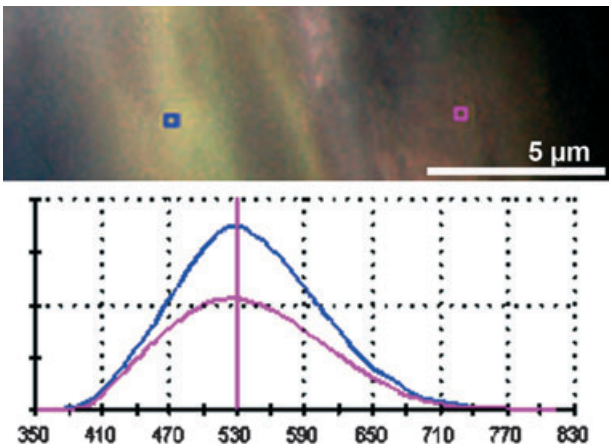

Fig. 4 *In vivo* bone labeling using only tetracycline (filter set 01, Zeiss). Note that the fluorescence colour mimics different colours in different regions of the bone, even though only one tetracycline is applied to this animal. It can be proven by spectral image analysis that the wavelength peak is identical for tetracycline (529 nm) in areas of different bone maturity [osteoid on the right (pink square and wavelength graph), mature bone on the left (blue square and graph)]. The ordinate displays the relative values of fluorescence intensity.

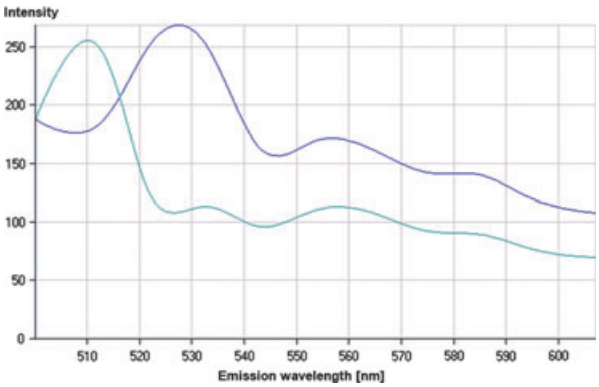

Fig. 5 Fluorescence spectra acquired by ACE (automatic component extraction). Two spectra can be clearly separated. The first spectrum with a peak of 510 nm corresponds to chlortetracycline, whereas the second spectrum with a peak at 529 nm corresponds to the emission of doxycycline, rolitetracycline and tetracycline.

as well as CLSM analysis confirmed the same wavelength peak and emission spectrum (Fig. 4).

All tetracycline derivates showed different fluorescence brightness, which could be quantified in a comparative manner by spectral image analysis. This was done during spectral acquisition using the intensity of the maximum peak wavelength. In descending order, tetracycline revealed the brightest fluorescence [relative intensity (ri) = 1], followed by demeclocycline (ri = 0.82), oxytetracycline (ri = 0.59), methacycline (ri = 0.55), rolitetracycline (ri = 0.34), chlortetracycline (ri = 0.24), and doxycycline (ri = 0.24). As a consequence, chlortetracycline and doxycycline were administered at a concentration of 60 mg kg^{-1} bodyweight, resulting in a brighter fluorescence. The measurements were performed in different spots ($n > 3$) and in different samples ($n > 3$) from one animal (the animal that received only a single tetracycline derivate).

Using different fluorochrome combinations, chlortetracycline could be reliably distinguished from all other fluorochromes (Figs 2, 5 and 6) by spectral imaging analysis and CLSM. The results of the two imaging modalities were comparable.

Individual depiction of any of the other tetracycline derivates was not possible because their wavelength spectra were too similar for the acquisition algorithm used.

Discussion

Tetracycline-based histological analysis of bone remodeling is an important technique for *in vivo* bone research, as tetracyclines are the only fluorochromes approved for human application (Parfitt et al. 2000; Arlot et al. 2005; Land et al. 2007). To date, only one study has addressed the question of whether it is possible to discriminate different tetracycline derivates in bone (Lindsay et al. 2006) and so far nobody has used spectral image analysis or confocal laser scanning microscopy for discrimination. Lindsay and co-workers observed slight colour differences in a bone-labeling study using double labeling with tetracycline and demeclotetracycline. Their conclusion was that both tetracycline derivates were distinguishable with the naked eye. However, using spectral imaging modalities in our study, a peak wavelength difference between these two tetracycline derivates of only 6 nm was found, and reliable discrimination was not possible using spectral camera, CLSM or the unaided human eye. In common with other studies, we found that the same tetracycline could appear as different colours to the naked eye (Rauch et al. 2006). It is most likely that this phenomenon is caused by the auto-fluorescence of differently calcified bone (Bachman & Ellis, 1965; Prentice, 1965; Del Castillo et al. 1989). Using modern image analysis methods, it can be shown that the peak wavelengths are identical, even if the colour looks slightly different to the human eye. The advantage of spectral image analysis techniques relates not only to the observer-independent reproducibility of the results but also to the fact that auto-fluorescence does not severely impair the investigation.

The spectral image analysis techniques used in this study not only assess the peak emission wavelength, but also the complete emission spectrum. Fluorochromes with identical emission wavelength peaks can therefore be distinguished even if all their spectra are different. This discrimination cannot be achieved with conventional fluorescence microscopy. As a consequence, it was expected to differentiate between more than two tetracycline derivates because their emission peaks varied between 506 and 547 nm. In histological studies at the cellular level, differentiation of emission peaks in the range of 10 nm is currently possible (Schieker et al. 2007). In histological sections we found that

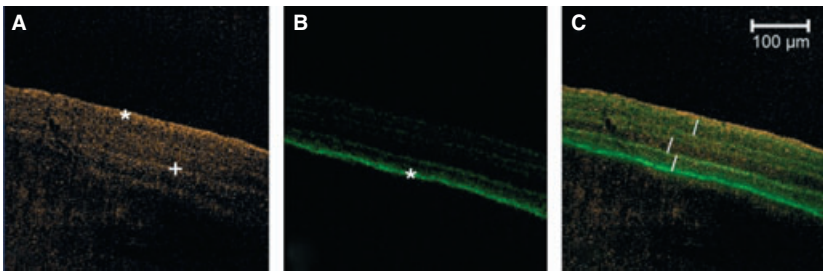

Fig. 6 Multichannel image of a polychrome bone labeling with eight tetracycline derivates after linear unmixing of a lambda stack based on the ACE analysis for two dyes as seen in Fig. 5. (A) Emission of doxycline (*) and rolitetracycline/tetracycline (+) which were administered consecutively. (B) Labelling of chlortetracycline (o) with a defined fluorescence due to the specific emission at 510 nm. (C) Multichannel image of (A) and (B).

distinction was possible in the range of 20 nm (Pautke et al. 2005). This is due to the fact that the fluorescence labels in histological sections and in particular in undecalcified bone samples do not seem to be as clearly defined as on the cellular level when immunofluorescence techniques are used. As spectral imaging is more sensitive to signal intensity compared with conventional fluorescence microscopy, the thickness of the histological sections can be reduced to 5 μm (Pautke et al. 2005). However, to facilitate comparison with conventional microscopy, this reduction was not done in this study.

Reliable and reproducible discrimination was only possible between chlortetracycline and other tetracycline derivates, allowing real *in vivo* double labeling of calcifying tissues in human patients. Further improvement could be achieved by reducing the region of interest and increasing the magnification and thus the spatial resolution. However, this approach gives detailed results with enormously large datasets, unsuitable for routine analysis. On the other hand, lower resolution images may not contain enough information to address clinical questions of bone metabolism and structure. The three-dimensional complexity of bone also has to be considered because regions where the labels are approximately perpendicular to the plane of section are most suitable for analysis.

CLSM, which has been established for bone analysis for many years, offers another way to overcome the problem of overlapping fluorescent regions because it allows a theoretical resolution of 1 μm along the *z*-axis (Jones et al. 2005; Pilolli et al. 2008). A confocal pinhole aperture excludes most of the light from the out-of-focus planes so that mainly light from in-focus objects reaches the detector (North, 2006). Thus every layer of the specimen can be measured separately and a 3D-image of the regions with fluorescent emission can be generated.

Our results show that the fluorescence intensities of the various tetracycline derivates are different. As fluorochromes exhibiting similar fluorescence intensities are more suitable for investigation (Schieker et al. 2004; Pautke et al. 2007), it is advisable to chose the derivates with the highest relative intensity. Therefore, we recommend tetracycline when intravenous or subcutaneous administration is planned. For oral administration, the good bioavailability of doxycycline [i.e. twice as high as that of tetracycline (Sakellari et al. 2000)], has to be considered (Nielsen & Gyrd-Hansen, 1996). Unexpectedly, minocycline exhibited no detectable *in vivo* fluorescence. A similar result has been reported previously by McEvoy, (1992). Nevertheless, a study by Gerlach reported the successful use of minocycline for histomorphometric bone labeling (Gerlach et al. 2002). A possible explanation for this discrepancy might be that a higher concentration was used and that the minocycline preparation and adminstration were performed differently. Whereas Gerlach and coworkers (2002) suspended minocycline in carboxymethylcellulose, we administered minocycline in aqueous solution using a nutrition tube at the same dosage as that for subcutaneous administration.

Conclusion

The fluorescent characteristics of eight different tetracyclines are presented. For real double labeling, tetracycline and chlortetracycline appear to be the most suitable choice; however, reliable discrimination requires the use of advanced spectral imaging modalities. A discrimination of a third tetracycline derivate might be possible in the near future using more sensitive spectral discrimination methods. No differences were observed between spectral imaging analysis and CLSM, rendering both methods equally suitable for spectral fluorescence analysis.

Acknowledgements

This study has been supported by the AO Research Fund Grant (S-06-72T) and the KKF (Kommission für Klinische Forschung) of the Technical University of Munich (KKF 37-06). The spectrometric analysis was performed at the Faculty for Physics of the LMU Munich in cooperation with Dr Hanna Engelke. The CLSM 510 META NLO (Zeiss, Germany), software and technical support were provided by the Light Microscopy Centre of the ETH Zurich with special help from Dr Justine Kusch and Dr Gabor Csucs.

References

Aaron JE, Makins NB, Francis RM, et al. (1984) Staining of the calcification front in human bone using contrasting fluorochromes *in vitro*. *J Histochem Cytochem* **32**, 1251–1261.

Arlot M, Meunier PJ, Boivin G, et al. (2005) Differential effects of teriparatide and alendronate on bone remodeling in postmenopausal women assessed by histomorphometric parameters. *J Bone Miner Res* **20**, 1244–1253.

Bachman CH, Ellis EH (1965) Fluorescence of bone. *Nature* **206**, 1328–1331.

Coen G, Ballanti P, Balducci A, et al. (2006) Renal osteodystrophy: alpha-Heremans Schmid glycoprotein/fetuin-A, matrix GLA protein serum levels, and bone histomorphometry. *Am J Kidney Dis* **48**, 106–113.

Degidi M, Scarano A, Piattelli M, et al. (2005) Bone remodeling in immediately loaded and unloaded titanium dental implants: a histologic and histomorphometric study in humans. *J Oral Implantol* **31**, 18–24.

Del Castillo P, Llorente AR, Stockert JC (1989) Influence of fixation, exciting light and section thickness on the primary fluorescence of samples for microfluorometric analysis. *Basic Appl Histochem* **33**, 251–257.

Freemont AJ, Hoyland JA, Denton J (2005) The effects of lanthanum carbonate and calcium carbonate on bone abnormalities in patients with end-stage renal disease. *Clin Nephrol* **64**, 428–437.

Frost HM (1963) Measurement of human bone formation by means of tetracycline labelling. *Can J Biochem Physiol* **41**, 31–42.

Frost HM (1969) Tetracycline-based histological analysis of bone remodeling. *Calcif Tissue Res* **3**, 211–237.

van Gaalen SM, Kruyt MC, Geuze RE, et al. (2010) Use of fluorochrome labels in *in vivo* bone tissue engineering research. *Tissue Eng Part B Rev* **16**, 209–217.

Gerlach RF, Toledo DB, Fonseca RB, et al. (2002) Alveolar bone remodelling pattern of the rat incisor under different functional conditions as shown by minocycline administration. *Arch Oral Biol* **47**, 203–209.

Harris WH (1960) A microscopic method of determining rates of bone growth. *Nature* **188**, 1038–1039.

Jones CW, Smolinski D, Keogh A, et al. (2005) Confocal laser scanning microscopy in orthopaedic research. *Prog Histochem Cytochem* **40**, 1–71.

Land C, Rauch F, Travers R, et al. (2007) Osteogenesis imperfecta type VI in childhood and adolescence: effects of cyclical intravenous pamidronate treatment. *Bone* **40**, 638–644.

Lindsay R, Cosman F, Zhou H, et al. (2006) A novel tetracycline labeling schedule for longitudinal evaluation of the short-term effects of anabolic therapy with a single iliac crest bone biopsy: early actions of teriparatide. *J Bone Miner Res* **21**, 366–373.

Maggiano C, Dupras T, Schultz M, et al. (2006) Spectral and photobleaching analysis using confocal laser scanning microscopy: a comparison of modern and archaeological bone fluorescence. *Mol Cell Probes* **20**, 154–162.

Malik Z, Dishi M, Garini Y (1996) Fourier transform multipixel spectroscopy and spectral imaging of protoporphyrin in single melanoma cells. *Photochem Photobiol* **63**, 608–614.

McEvoy GK (1992) *AHFS Drug Information*. Bethesda: American Society of Hospital Pharmacists Inc.

Nielsen P, Gyrd-Hansen N (1996) Bioavailability of oxytetracycline, tetracycline and chlortetracycline after oral administration to fed and fasted pigs. *J Vet Pharmacol Ther* **19**, 305–311.

North AJ (2006) Seeing is believing? A beginners' guide to practical pitfalls in image acquisition. *J Cell Biol* **172**, 9–18.

Parfitt AM, Travers R, Rauch F, et al. (2000) Structural and cellular changes during bone growth in healthy children. *Bone* **27**, 487–494.

Pautke C, Vogt S, Tischer T, et al. (2005) Polychrome labeling of bone with seven different fluorochromes: enhancing fluorochrome discrimination by spectral image analysis. *Bone* **37**, 441–445.

Pautke C, Tischer T, Vogt S, et al. (2007) New advances in fluorochrome sequential labelling of teeth using seven different fluorochromes and spectral image analysis. *J Anat* **210**, 117–121.

Pautke C, Bauer F, Tischer T, et al. (2009) Fluorescence-guided bone resection in bisphosphonate-associated osteonecrosis of the jaws. *J Oral Maxillofac Surg* **67**, 471–476.

Pautke C, Bauer F, Bissinger O, et al. (2010) Tetracycline bone fluorescence: a valuable marker for osteonecrosis characterization and therapy. *J Oral Maxillofac Surg* **68**, 125–129.

Pilolli GP, Lucchese A, Maiorano E, et al. (2008) New approach for static bone histomorphometry: confocal laser scanning microscopy of maxillo-facial normal bone. *Ultrastruct Pathol* **32**, 189–192.

Prentice AI (1965) Bone autofluorescence and mineral content. *Nature* **206**, 1167.

Rahn B (1976) *Die polychrome Sequenzmarkierung Intravitale Zeitmarkierung zur tierexperimentellen Analyse der Knochen- und Dentinbildung*. Freiburg: Habilitationsschrift.

Rauch F (2006) Watching bone cells at work: what we can see from bone biopsies. *Pediatr Nephrol* **21**, 457–462.

Rauch F, Travers R, Parfitt AM, et al. (2000) Static and dynamic bone histomorphometry in children with osteogenesis imperfecta. *Bone* **26**, 581–589.

Rauch F, Travers R, Glorieux FH (2006) Cellular activity on the seven surfaces of iliac bone: a histomorphometric study in children and adolescents. *J Bone Miner Res* **21**, 513–519.

Rauch F, Travers R, Glorieux FH (2007) Intracortical remodeling during human bone development – a histomorphometric study. *Bone* **40**, 274–280.

Sakellari D, Goodson JM, Kolokotronis A, et al. (2000) Concentration of 3 tetracyclines in plasma, gingival crevice fluid and saliva. *J Clin Periodontol* **27**, 53–60.

Schieker M, Pautke C, Reitz K, et al. (2004) The use of four-colour immunofluorescence techniques to identify mesenchymal stem cells. *J Anat* **204**, 133–139.

Schieker M, Pautke C, Haasters F, et al. (2007) Human mesenchymal stem cells at the single-cell level: simultaneous seven-colour immunofluorescence. *J Anat* **210**, 592–599.

Schnitzler CM, Mesquita JM (2006) Cortical bone histomorphometry of the iliac crest in normal black and white South African adults. *Calcif Tissue Int* **79**, 373–382.

Smith IO, Ren F, Baumann MJ, et al. (2006) Confocal laser scanning microscopy as a tool for imaging cancellous bone. *J Biomed Mater Res B Appl Biomater* **79**, 185–192.

Togawa D, Lieberman IH, Bauer TW, et al. (2005) Histological evaluation of biopsies obtained from vertebral compression fractures: unsuspected myeloma and osteomalacia. *Spine* **30**, 781–786.